Iranian Journal of Materials Forming 13 (3) (2026) 12-25

Online ISSN: 2383-0042

IJMF

Iranian Journal of Materials Forming

Journal Homepage: http://ijmf.shirazu.ac.ir

Research Article

Investigation of Globularization and Mechanical Behavior of Ti-8Al-1Mo-1V Alloy During Post-Deformation and Heat Treatment

Gholamreza Ebrahimi[1*], Zahra Mirzaie[2] and Hamidreza Ezatpour[3†]

[1] Department of Materials Science and Engineering, Faculty of Engineering, Ferdowsi University of Mashhad, Mashhad, Iran
[2] Department of Materials and Polymers Engineering, Faculty of Engineering, Hakim Sabzevari University, Sabzevar, Iran
[3] Department of Materials Engineering, Vali-e-Asr University of Rafsanjan, Rafsanjan, Iran

ARTICLE INFO

Article history:

Received: 1 November 2025
Reviewed: 22 November 2025
Revised: 16 December 2025
Accepted: 21 December 2025

Keywords:

Ti-811 alloy
Hot compressive test
Heat treatment
Globularization
Mechanical properties

Please cite this article as:

Ebrahimi, G., Mirzaie, Z., & Ezatpour, H. (2026). Investigation of globularization and mechanical behavior of Ti-8Al-1Mo-1V alloy during post-deformation and heat treatment. *Iranian Journal of Materials Forming*, *13*(3), 12-25. https://doi.org/10.22099/IJMF.2026.54721.1360

ABSTRACT

In this study, the effect of hot compression and subsequent heat treatment on α globularization and mechanical properties of Ti-8Al-1Mo-1V (Ti-811) alloy with an initial lamellar microstructure was investigated. Heat treatment was performed on hot-deformed samples (at 1000 °C and 0.001 s^{-1}), at temperatures of 800, 850, and 900 °C for durations ranging from 1 h to 5 h. The results showed that the microstructural changes depended on the temperature and time of heat treatment and globular α phase fraction increased with increasing time and temperature. By increasing the heat treatment temperature from 800 °C to 900 °C for 5 h, the volume fraction of globular α phase increased from 68% to 79% and the aspect ratio decreased from 7.2 to 6.2. Microstructural studies showed that the globularization mechanism was controlled by boundary splitting, interface migration, and Ostwald growth. At lower temperatures of 800 °C and 850 °C, the dominant mechanism was boundary splitting by the shearing of α layers, which depended on the amount of pre-strain. At the higher temperature of 900 °C, globularization was controlled by interface migration and Ostwald growth, which were diffusion processes and dependent on heat treatment time. The static globurization kinetics of Ti-811 during heat treatment was well modeled by the modified JMRE equation, with a correlation coefficient (R) of 0.97 and the mean absolute relative error (MARE) of 7.19%. A punching test was applied to evaluate the mechanical properties of the deformed and heat-treated samples. The maximum shear strength and elongation were obtained at 900 °C and a holding time of 2 h, which were equal to 695 MPa and 1.1, respectively.

1. Introduction

Titanium (Ti) alloys are widely used in the automotive, aerospace, and medical industries due to high specific strength, desirable toughness, and outstanding fatigue properties [1-6]. To further improve their mechanical performance, the processes such as hot forging and heat

* Corresponding author
E-mail address: r.ebrahimi@um.ac.ir (G. Ebrahimi)

† Corresponding author
E-mail address: h.ezatpour@vru.ac.ir (H. Ezatpour)
https://doi.org/10.22099/IJMF.2026.54721.1360

treatment are usually employed. The mechanical properties of Ti alloys are strongly depend on their microstructural features, including the volume fraction, morphology, distribution and orientation of the α phase [3, 7]. In Ti alloys, α phase mainly exhibits two distinct morphologies: lamellar and equiaxed/globular [8]. Each morphology has distinct properties, making it suitable for different applications [9]. Lamellar microstructures provide moderate strength and good resistance to high-temperature creep and fracture, whereas equiaxed/globular microstructures offer a better balance between strength and toughness.

Globularization treatment for achieving a globular microstructure includes two types of dynamic, which occurs in the α + β region during deformation, and static globularization, which takes place during post-deformation heat treatment in the α + β region [10-13]. To achieve a fully globular microstructure through dynamic process requires imposing a very high strain, typically in the range of 1.34 to 5.36, which is difficult to obtain using conventional forming processes [11, 14]. Therefore, static globularization during heat treatment is often introduced as an additional step following deformation. Stefansson et al. [15] investigated the static globularization of forged Ti-6Al-4V alloy at 900 °C and 955 °C for various times. They concluded that the kinetic of static globularization of lamellar α are mainly influenced by the amount of pre-strain and the heat treatment temperature, rather than the deformation temperature. Park et al. [16] investigated the static globularization of Ti-6Al-2Sn-4Zr-2Mo-0.1Si alloy, after hot compression test at 900 °C, followed by heat treatment at 955 and 980 °C. Their results indicated that strain rate, temperature, and holding time are the main effective factors. Stefansson et al. [17] further reported that globularization occurs during the formation of α/α sub-grain boundaries, and subsequent boundary splitting. Chong et al. [18] showed that splitting and growth of the α phase are the main mechanisms of dynamic globularization during hot deformation of Ti-64 alloy at 950-900 °C. They also confirmed that grain boundary migration promotes globularization during post-deformation heat treatment. Zherebtsov et al. [19] stated that at 800 °C, the transformation from a lamellar microstructure to a globular one is initially controlled by grain boundary splitting, followed by further globularization through interface migration mechanism.

Previous studies have provided valuable insights into both dynamic and static globularizations in Ti alloys, particularly in Ti-6Al-4V alloy. However, a comprehensive consideration of static globularization, including the simultaneous effect of heat-treatment temperature and time, as well as the influence of α phase volume fraction and aspect ratio on shear properties remains limited.

In the present study, the static globularization behavior and mechanical properties of Ti-811 alloy hot-compressed at 1000 °C and a strain rate of 0.001 s^{-1} were investigated following heat treatment (in the α + β region) at different temperatures of 800 °C to 900 °C for holding times between 1 and 5 h. For this purpose, the microstructures of Ti-811 alloy at different conditions are carefully examined to identify the microstructural changes and the main mechanisms of globularization. The static globularization kinetic is also modeled by the JMRE constitutive equation. Punching tests on thin sheets were applied to characterize the elastic-plastic mechanical behavior of the Ti-811 alloy under complex stress state conditions [20-22].

2. Materials and Methods

The material used in this study is Ti-811 alloy, whose nominal chemical composition is reported in Table 1. Ti-811 alloy contains 35.7 wt.% Al (as an α-phase stabilizer) and a total of 1.5 wt.% V and Mo (as β-phase stabilizers) and is therefore classified as a near-α alloy.

Table 1. Chemical composition of Ti-811 alloy (wt.%)

Al	Mo	V	Fe	C	Ti
7.35	0.75	0.75	0.3	0.08	Balance

Using differential thermal analysis (DTA), an endothermic peak was observed at a temperature of about 1030 °C, which indicates the β transformation temperature (Fig. 1(a)). Fig. 1(b) shows the phase diagram of the studied alloy in the temperature range of

600-1100 °C, which was drawn using JMatPro software. A single β phase region is present at temperatures above 1005 °C, and with decreasing temperature, a dual-phase region of α and β appears. The phase transformation temperature obtained from JMatPro software is in good agreement with the value obtained from DTA (1030 °C) for the studied alloy.

Before deformation, a homogenization heat treatment was carried out at a temperature above the β transformation temperature, at 1050 °C for 1 h, followed by rapid water quenching. The homogenization temperature was chosen slightly higher than the transformation temperature (by about 10 °C) to prevent the growth of β grains with increasing temperature. The microstructure of the sample after the homogenization treatment consists of α martensitic within a β matrix. The thickness of the α martensitic fine layers is about 0.3 µm (Fig. 2).

The cylindrical samples with a height of 12 mm and a diameter of 8 mm were cut from the homogenized material using wire cutting. Hot compression tests were

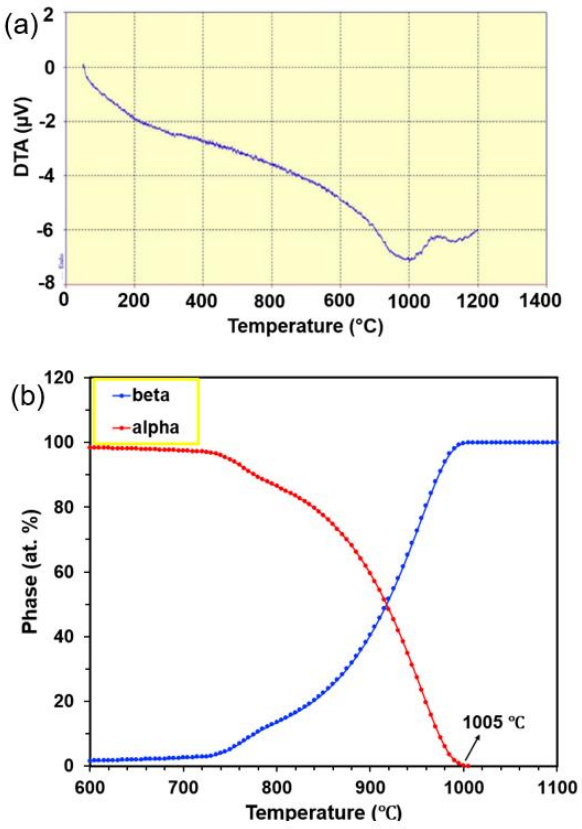

Fig. 1. (a) DTA analysis and (b) phase changes versus temperature of Ti-811 alloy.

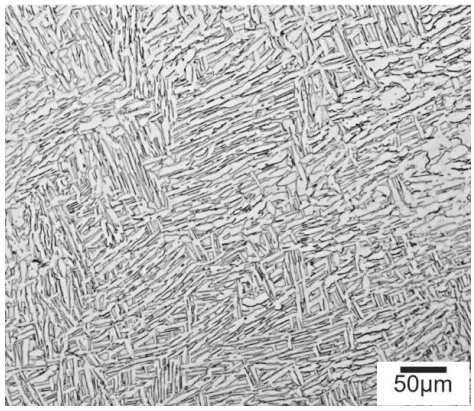

Fig. 2. Microstructure of Ti-811 alloy after homogenization at 1050 °C for 1 h.

carried out at a temperature of 1000 °C and a strain rate of 0.001 s^{-1} up to a true strain of 0.9 using a ZWICK Z250 testing machine with a capacity of 25 tons, equipped with a resistance furnace with an accuracy of ± 5 °C. It should be mentioned that plastic deformation at low strain rate is generally considered isothermal, whereas deformation at high strain rate leads to a transition from isothermal to adiabatic conditions. The true strain of 0.09 in the hot compression test was selected to induce sufficient deformation in the specimen for activation of microstructural mechanisms such as dislocation rearrangement and α globularization. This level of strain enables the analysis of the mechanical behavior and microstructure evolution prior to the annealing heat treatment and is comparable to previous studies on α + β titanium alloys [23-25].

To preserve the microstructure, the samples were immediately quenched in water. To reduce friction during high temperature deformation, mica sheets with a thickness of approximately 0.1 mm were placed between the sample surface and the jaws. Then, in order to achieve globular α microstructures, the samples were heat treated at temperatures of 800, 850, and 900 °C for 1, 2, 3, 4, and 5 h under an argon atmosphere. The heating rate was 100 °C/min. A schematic illustration of the experimental procedure is shown in Fig. 3.

The mechanical properties of Ti-811 alloy were evaluated using a punching test. The results of punching tests can be used to further validate the models of mechanical behavior of materials developed based on

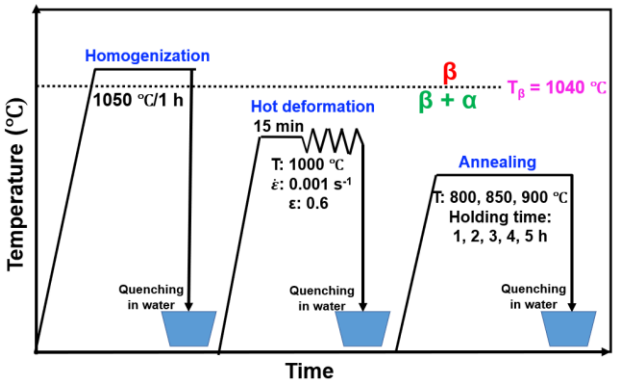

Fig. 3. Schematic illustration of the experimental steps of this study.

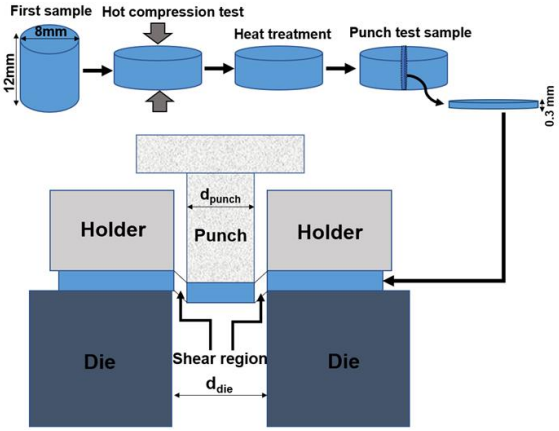

Fig. 4. Schematic illustration of the punching process.

uniaxial loading data. Accordingly, the shear strength of deformed and subsequently heat-treated samples was determined using a shear punching test under different conditions. From the aforementioned samples, sheets with a thickness of 0.3 mm were cut by wire cutting. The punching test was performed using a mandrel with a diameter of 3 mm (d_{punch}), a die diameter (d_{die}) of 3 ± 0.03 mm and a punch speed of 0.72 mm/min using a ZWICK universal press. A graphite lubricant was applied to reduce friction between the sample, die and mandrel. Five samples were tested for each condition to ensure data reliability. A schematic diagram of the punching test is shown in Fig. 4. The instantaneous force (P) and punch displacement (Δ) were recorded by a computer. The shear stress (τ) and strain (δ) were calculated using the following equations [26, 27].

$$\tau = P/(\pi dt) \quad (1)$$

$$\delta = \Delta/t \quad (2)$$

Where, d is defined as $(d_{punch} + d_{die})/2$, (d_{punch} and d_{die} are punch and die diameters) and t is the sample thickness. It should be noted that δ represents an engineering approximation and is used to compare the relative strain levels between the samples.

For microstructural analysis, after standard sample preparation, the samples were etched using Kroll solution containing 92% H_2O + 2% HF + 6% HNO_3. An OLYMPUS-BX41M-LED optical microscope was used for microstructural images. ImageJ analysis software was employed to determine the volume fraction and aspect ratio of α particles, with 75-100 particles measured to obtain an average value. According to Ref. [10], α particles with an aspect ratio (length/thickness) of less than 2.5 are considered globular. Three micrographs were analyzed for each condition.

3. Results and Discussion

3.1. Flow stress curve and microstructure after hot deformation

Fig. 5 shows the true stress-true strain curve of Ti-811 alloy deformed at a temperature of 1000 °C and an applied strain rate of 0.001 s^{-1} up to a true strain of 0.9. It is observed that the stress level reaches a maximum value with a slight increase in the applied strain due to the production and accumulation of dislocations (work hardening step). With a further increase in strain, the flow stress level decreases and work softening occurs. Subsequently, the flow stress reaches a stable state as a result of a balance between work hardening and work softening mechanisms. This type of stress-strain curve has been reported during hot deformation of Ti alloys in the α + β region [23, 28]. The softening of the flow stress can be attributed to several factors, such as deformation heating and microstructural evolution [4, 29, 30]. Since the applied strain rate is low, the effect of deformation heating can be neglected [4]. Deformation in the dual-phase region of α + β leads to microstructural evolution through (i) changes in the volume fraction of the α and β phases due to dynamic phase transformation, and (ii)

changes in the morphology of the α phase during globularization, which can be examined by microstructural observations [4, 18, 23, 31]. A notable point in the flow curve of the hot-deformed Ti-811 alloy is the presence of serrations, which are associated with flow instability. Serrated flow and discontinuous yielding have also been reported in other Ti alloys such as IMI834 [32], Ti-64 [12, 33, 34], and Ti-811 [35].

The microstructure of the deformed sample at 1000 °C and 0.001 s^{-1} (Fig. 5(b)) shows that, compared with the homogenized sample (Fig. 2), the thickness of the α layers has increased from approximately 0.3 µm to 7.5 µm and some globular α particles of about 17% are also observed. Bending and kinking of the α phase occur during deformation [36]. However, the morphology of the α phase has still maintained its layered structure and the globularization is at a low level. Wanjara et al. [32] showed that hot deformation of the IMI834 alloy leads to strain localization, the formation of shear bands and further splitting of α layers. Zherebtsov et al. [19] reported that flow softening in stress-strain curves occurs due to kinking of α layers, rearrangement of dislocations, and the formation of sub-grain boundaries in the α phase.

3.2. Microstructure of deformed Ti-811 alloy after heat treatment at 800 °C and 850 °C

Fig. 6 shows the microstructures of samples heat treated at 800 °C for 1 h to 5 h. Compared with the deformed sample (Fig. 5(b)), the fraction of globular α phase increases after heat treatment at 800 °C, through the

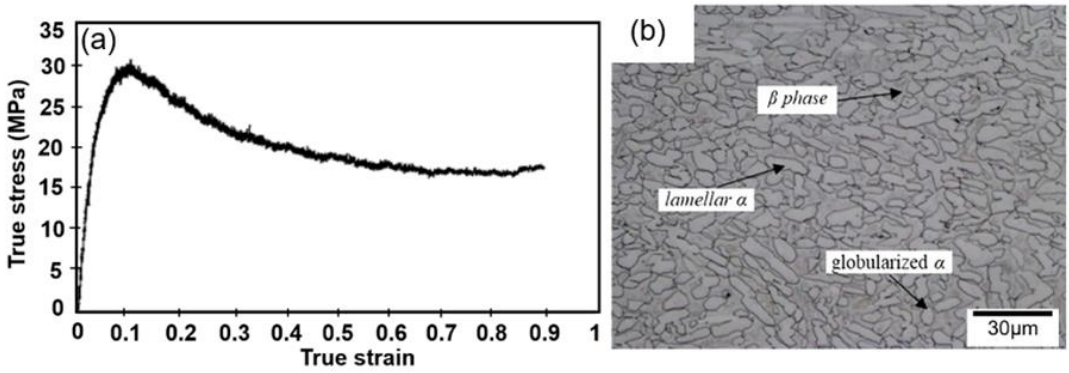

Fig. 5. (a) True stress-true strain curve of the Ti-811 alloy deformed at 1000 °C and 0.001 s^{-1} and (b) microstructure of the Ti-811 alloy after hot deformation under the same conditions.

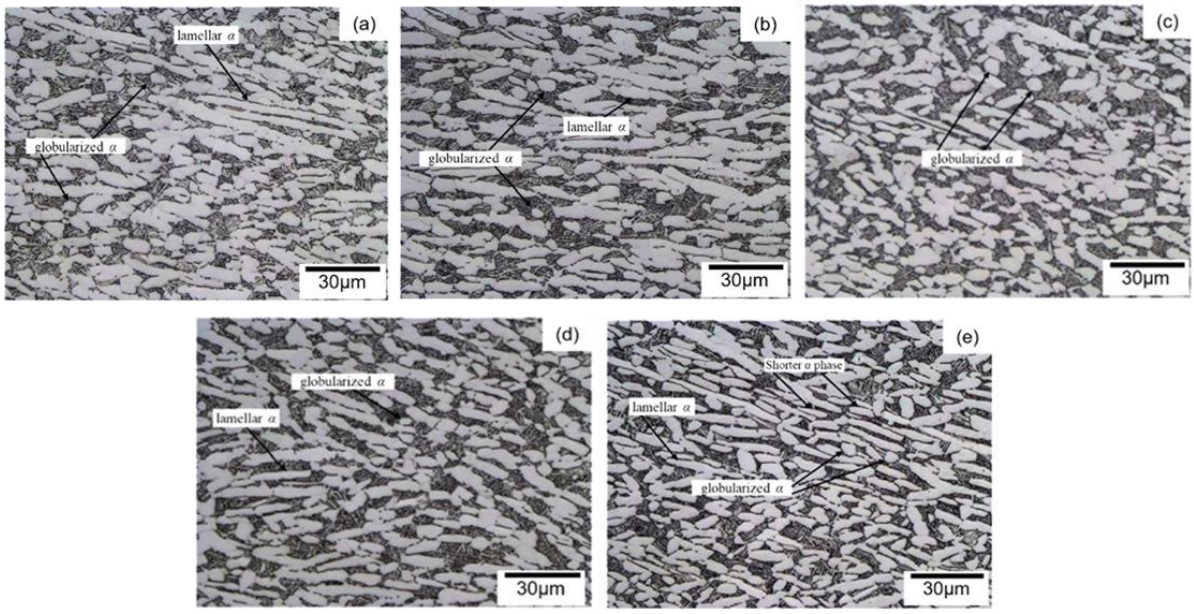

Fig. 6. Microstructures of the Ti-811 alloy after heat treatment at 800 °C for (a) 1 h, (b) 2 h, (c) 3 h, (d) 4 h, and (e) 5 h.

boundary splitting mechanism. Bending and kinking of α layers are also observed in some regions. With increasing heat treatment time from 1 h to 5 h, the thickness of the α layers decreases, while the boundary splitting rate increases. This confirms that finer α layers are divided more easily and rapidly during globularization [37, 38]. Consequently, the fraction of globular α phase increases from 31% for 1 h to 67% after 5 h of heat treatment.

Fig. 7 shows the microstructures of samples heat treated at 850 °C for durations ranging from 1 h to 5 h. The fraction of globular α phase increases with increasing temperature from 800 °C to 850 °C. The results further indicate that the fraction of globular α phase at 850 °C increases from 38% after 1 h to 76% for 5 h (Fig. 8). As the temperature increases, it provides more driving force for the penetration of the β phase, which facilitates the splitting and globularizing of the α layers. In other words, at both 800 °C and 850 °C, globularization of the α layers mainly occurs through the boundary splitting mechanism.

To better understand the globularization mechanism at 800 °C and 850 °C, the SEM image of the sample heat treated at 850 °C for 4 h is shown in Fig. 9. Regions A, B, C indicate the initial stages of α layer splitting. It is observed that in region A, splitting of the α layer occurs faster than in regions B and C. Regions B and C are not completely separated during deformation and subsequent heat treatment, likely due to insufficient energy. The lamellar microstructure in dual-phase alloys is thermodynamically unstable due to its large surface area. The energy stored during deformation increases at faults site and interfaces due to the accumulation of dislocations [13]. These dislocations promote atomic diffusion, leading to the formation of grooves on the layers surface, which develop the boundary splitting mechanism.

3.3. Microstructure of deformed Ti-811 alloy after heat treatment at 900 °C

Fig. 10 shows the microstructures of the samples heat treated at 900 °C for 1 h to 5 h. Thicker layers are observed in the microstructures of the samples heat treated at all times as compared to those at 800 °C and 850 °C. Also, a larger fraction of globular α phase is observed with increasing heat treatment time from 1 h to 5 h (Fig. 11). A distinctive and notable feature of the microstructure at 900 °C is the presence of coarser α phase particles compared to those at 800 °C and 850 °C. Results illustrate that with increasing heat treatment temperature and time, the main mechanism of globularization changes from boundary splitting (globularization mechanism at 800 °C and 850 °C) to coarsening at 900 °C. The coarsening of the α phase occurs by two mechanisms: termination migration and Ostwald ripening. The mechanisms of termination migration and Ostwald ripening are processes dependent

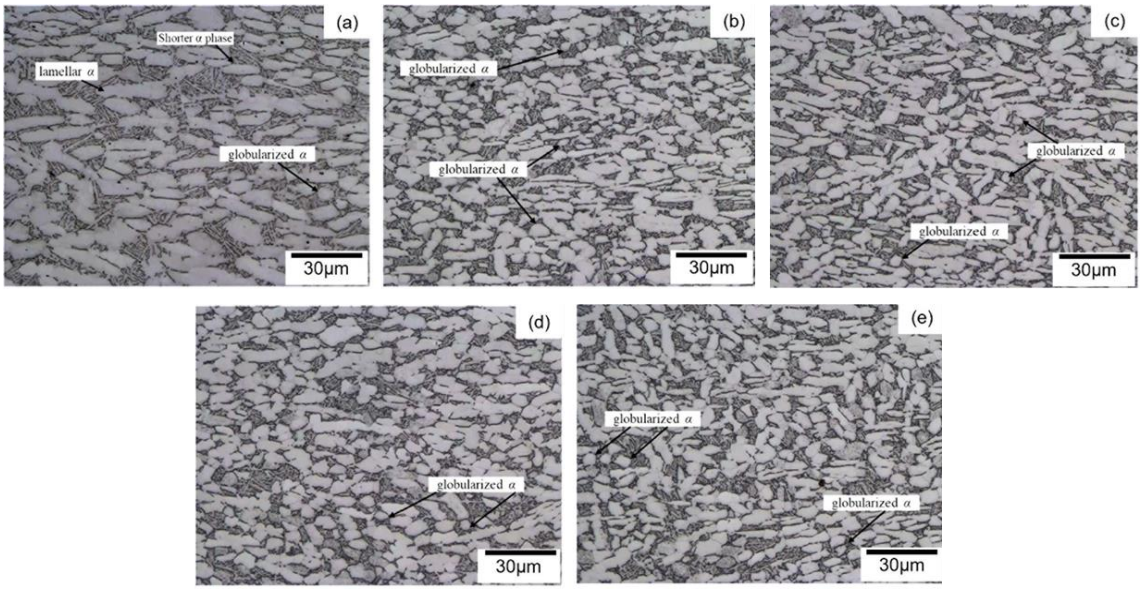

Fig. 7. Microstructures of Ti-811 alloy after heat treatment at 850 °C for (a) 1 h, (b) 2 h, (c) 3 h, (d) 4 h, and (e) 5 h.

on the atomic diffusion of elements that are strongly affected by the heat treatment temperature and time [10]. The driving force for these processes is provided by the difference in energy gradient at different positions within an α particle or between different α particles. The termination migration mechanism is influenced by the potential energy difference between points with different curvatures in the α layers. In areas with greater curvature, there is a higher potential energy and the diffusion of atoms occurs more easily, which leads to the formation of a chemical potential difference between the tip and the flat surface. As a result, solute atoms diffuse from the tip to the flat part of the α layer, which causes the dissolution of the tip part and the coarsening of the α layer. In the Ostwald growth mechanism, the coalescence of smaller particles and the formation of larger particles reduce the free energy of the system. Small α phase particles have a higher Gibbs free energy compared to larger particles. The energy difference between small and large particles provides the necessary driving force for the coalescence of small α particles and the formation of large α particles. Ostwald growth is accompanied by a decrease in the number and an increase in size of α particles.

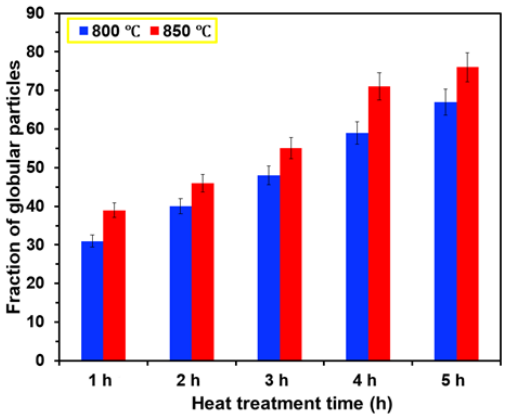

Fig. 8. Volume fraction of globular α phase at 800 °C and 850 °C for different heat treatment times.

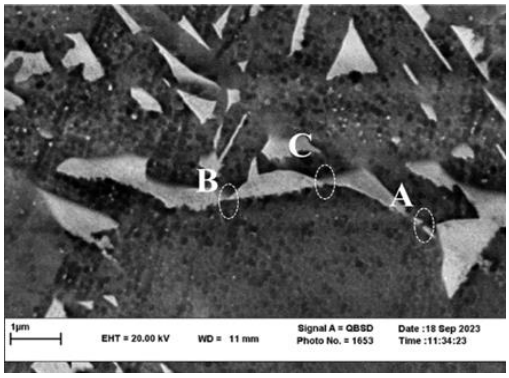

Fig. 9. SEM image of heat-treated Ti-811 alloy at 850 °C for 4 h.

By comparing the microstructures of the heat-treated samples at 800, 850, and 900 °C at different times from 1 h to 5 h, it can be concluded that, at all temperatures, with increasing heat treatment time, the fraction of the globular α phase increases with the highest value at 5 h (Figs. 8 and 11). With increasing heat treatment temperature from 800 °C to 900 °C, the aspect ratio of α particles decreases from 7.2 to 6.2, which can be attributed to globularizing and coarsening of these

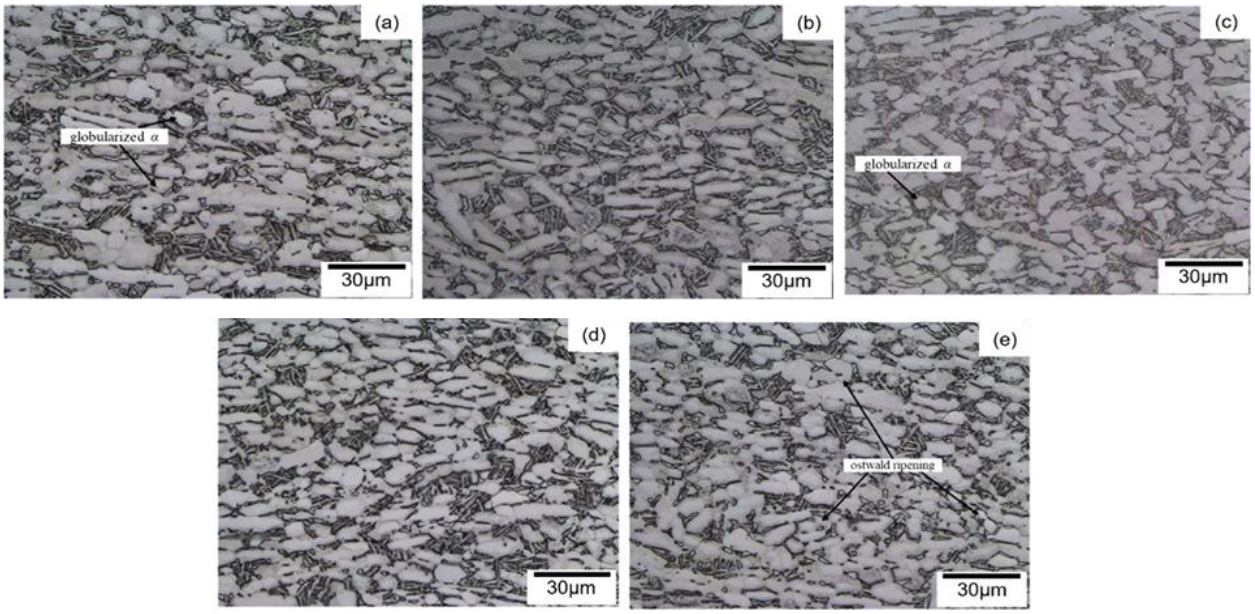

Fig. 10. Microstructures of Ti-811 alloy after heat treatment at 900 °C for (a) 1 h, (b) 2 h, (c) 3 h, (d) 4 h, and (e) 5 h.

(Fig. 12). Such observations are in agreement with reported results for Ti-64 [17], Ti-6Al-2Sn-4Zr-2Mo-0.1Si [16], and Ti-17 [10] alloys. Xu et al. [10] reported that boundary splitting is a rapid process which occurs at the initial stages of heat treatment. In contrast, microstructure coarsening due to interface migration and Ostwald mechanism is affected by heat treatment temperature and geometrical shape, which occurs in longer times of heat treatment.

It is observed that the globularization fraction of the α phase in the studied samples does not exceed 80%, even after 5 h of heat treatment at 900 °C. This response is typical for near-α Ti alloys such as Ti-811, since the limited fraction of the β phase reduces atomic diffusivity and thereby restricts the globularization process. The β phase provides fast diffusion pathways for atoms, particularly during deformation and globularization. When the β fraction is low, the diffusion of alloying elements such as Al and V (or other substitutional elements) becomes sluggish, which delays the transformation of α lamellae into a fully globularized morphology. Consequently, even after 5 h of heat treatment, some α layers remain thin, which prevents the increase in the globularization fraction. In contrast, Ti-64 alloy is an α+β-Ti alloy with a higher content of β phase, which offers more diffusion pathways and thus promotes a higher globularization fraction. Stefansson et al. [15] reported that globularization fraction of 90-95% can be achieved in Ti-64 alloy. Similarly, in the near-α Ti-17 alloy, which contains a larger β phase fraction compared to Ti-811 alloy, the globularization fraction can be achieved at approximately 85-90% [10]. Therefore, the behavior observed in Ti-811 alloy is consistent with diffusion-controlled mechanisms and microstructural evolution.

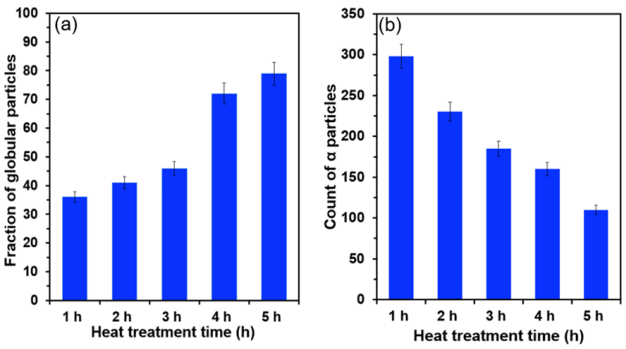

Fig. 11. Plots of (a) fraction and (b) number of globular α particles versus heat treatment time at 900 °C.

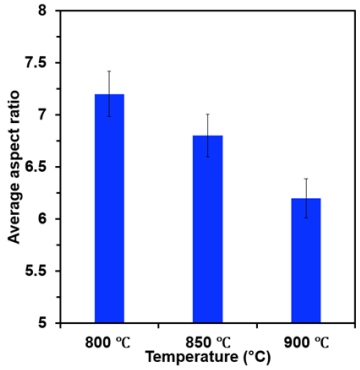

Fig. 12. Average aspect ratio of the α phase at different temperatures of 800, 850, and 900 °C for 5 h.

3.4. Globularization kinetics

The dynamic globularization kinetics of TA15 [39], TC11 [40], and BT25 [41] alloys have been quantitatively analyzed, and the results demonstrate that the Avrami equation can effectively describe this process. In addition, post-deformation/heat treatment can significantly promote the globularization of the α phase. Accordingly, the static globularization kinetics of TC11 [42], Ti-6Al-4V [15], TA15 [43], and TC17 [44] alloys have also been systematically investigated. These studies indicate that the static globularization is accelerated with increasing pre-strain and heat treatment temperature. Owing to similarities between static globularization and static recrystallization, the kinetics of this process can also be described by the JMAK equation [43]. In the present work, a modified JMAK model is developed to characterize static globularization kinetics. The basic form of this model is expressed as:

$$f = 1 - exp(-k't^n) \quad (3)$$

Where f is the globularization fraction, k' is the globularization rate constant, n is the Avrami exponent, and t is the heat-treatment time. However, static globularization is a complex process controlled by pre-strain, strain rate, heat-treatment temperature and time. Eq. (3) accounts only for the influence of time; therefore, a modified JMAK model is used as:

$$f = 1 - exp(-k'(\frac{t}{t_{0.5}})^n) \quad (4)$$

Where $t_{0.5}$ represents the time required to reach 50% globularization. This parameter is mainly influenced by pre-strain, strain rate, and heat treatment temperature, and can be expressed as:

$$t_{0.5} = A'\varepsilon^{-a}\dot{\varepsilon}^{-p}\, exp(\frac{Q}{RT}) \quad (5)$$

Where A' is a material constant, and a and p are constants. By substituting $t_{0.5}$ into Eq. (4) and taking the logarithm of both sides, the following relationship is obtained:

$$ln\, ln(\frac{1}{1-f}) = na\, ln\, \varepsilon + n\, ln\, t + np\, ln\, \dot{\varepsilon} - n\, ln\, A' + ln\, k' - n(\frac{Q}{RT}) \quad (6)$$

To simplify the model and consider simultaneously the effects of pre-strain, strain rate, and heat treatment temperature and time, it is assumed that a and p are equal to 1. In this case, Eq. (7) is obtained as:

$$ln\, ln(\frac{1}{1-f}) = n\, ln(\varepsilon\dot{\varepsilon}t) - n\, ln\, A' + ln\, k' - n(\frac{Q}{RT}) \quad (7)$$

Where, the term $ln\ k'$ - $n\ ln\ A'$ - $n(Q/RT)$ can be considered a constant when the heat treatment temperature is fixed. Therefore, a linear fitting method can be used to determine the relationship between $ln\, ln(1/1-f)$ vs. $ln(\varepsilon\dot{\varepsilon}t)$. Quantitative data at the heat treatment temperature are substituted into Eq. (7), and the fitting result are shown in Fig. 13.

The slope and intercept values of Fig. 13(a) are obtained as 0.73 and 1.42, respectively. Therefore, Eq. (8) indicating the static globularization kinetics of Ti-811 alloy at 900 °C can be presented as:

$$f = 1 - exp(-exp(0.73\, ln(\varepsilon\dot{\varepsilon}t) + 1.42)) \quad (8)$$

The comparison between the predicted values (obtained from Eq. (8)) and the experimental measurements is shown in Fig. 13(b). The correlation coefficient (R = 0.97) and the mean absolute relative error (MARE = 7.19%) confirm the high predictive accuracy of the modified JMAK model. Therefore, the model can reliably describe the influence of pre-strain, strain rate, and heat-treatment time on the static globularization behavior of the α phase in Ti-811 alloy.

3.5. Mechanical properties of Ti-811 alloy at different heat treatment conditions

The punching shear testing was used to analyze the mechanical properties of Ti-811 alloy under different conditions. This process consists of three stages: (1) elastic deformation, (2) plastic deformation, and (3) fracture and separation (Fig. 14). In the initial step of the punching process (stage 1), elastic deformation accommodated by different modes such as tension, compression and bending. With further penetration of the punch, the pressure applied to the upper surface of the specimen increases, while the lower surface slides

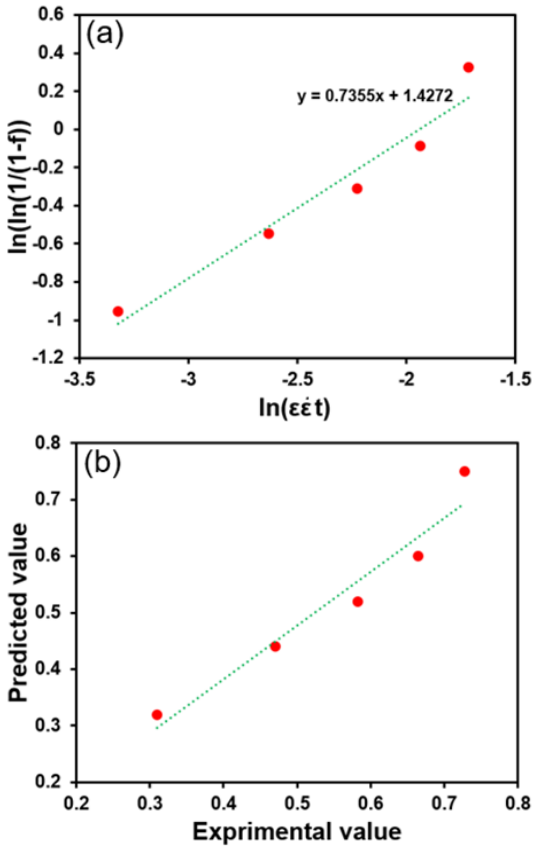

Fig. 13. (a) Relationship between $ln\, ln(\frac{1}{1-f})$ vs. $ln(\varepsilon\dot{\varepsilon}t)$ and (b) correlation between experimental values and those calculated using Eq. (8).

into the die. With further penetration of the punch, the stress increases up to the yield stress level, where plastic deformation (bending and tensile) occurs until it reaches a maximum point, and strain hardening occurs in this region (stage 2). In the failure and separation stage (stage 3), when punch penetration continues, microcracks form around the shear edge and grow into the sheet surface.

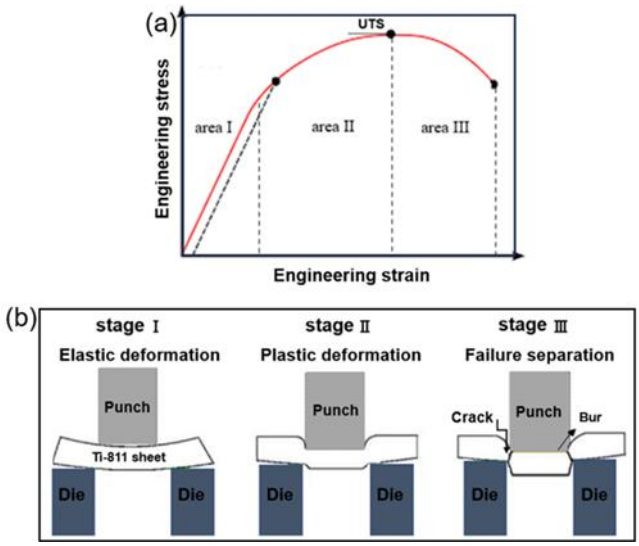

Fig. 14. Schematic image of (a) the stress-strain curve and (b) shear punching test stages.

When the upper and lower cracks overlap, the plate breaks and separates [26]. The stages shown in Fig. 14(a) are corresponding to the nature of the engineering stress-engineering strain curves.

The shear stress versus normal displacement curves and the maximum values of stress and strain of Ti-811 alloy at different conditions are shown in Fig. 15. The change in the microstructural characteristics of the α phase in different conditions of deformation and heat treatment determines the difference in the punching test curves.

The maximum stress and the corresponding strain are shown in Fig. 15(b, c). The punch test result of the sample deformed at 1000 °C and 0.001 s^{-1} shows that the stress increases with increase in strain and suddenly drops after reaching a maximum stress of 680 MPa and a strain of about 0.9. In the samples heat treated at temperatures of 800 °C and 900 °C for times of 2 h and 5 h, the highest shear strength and maximum strain are obtained at temperature of 900 °C and a time of 2 h, which are equal to 695 MPa and 1.1, respectively. It has been reported that globularization in Ti alloys delays the start of

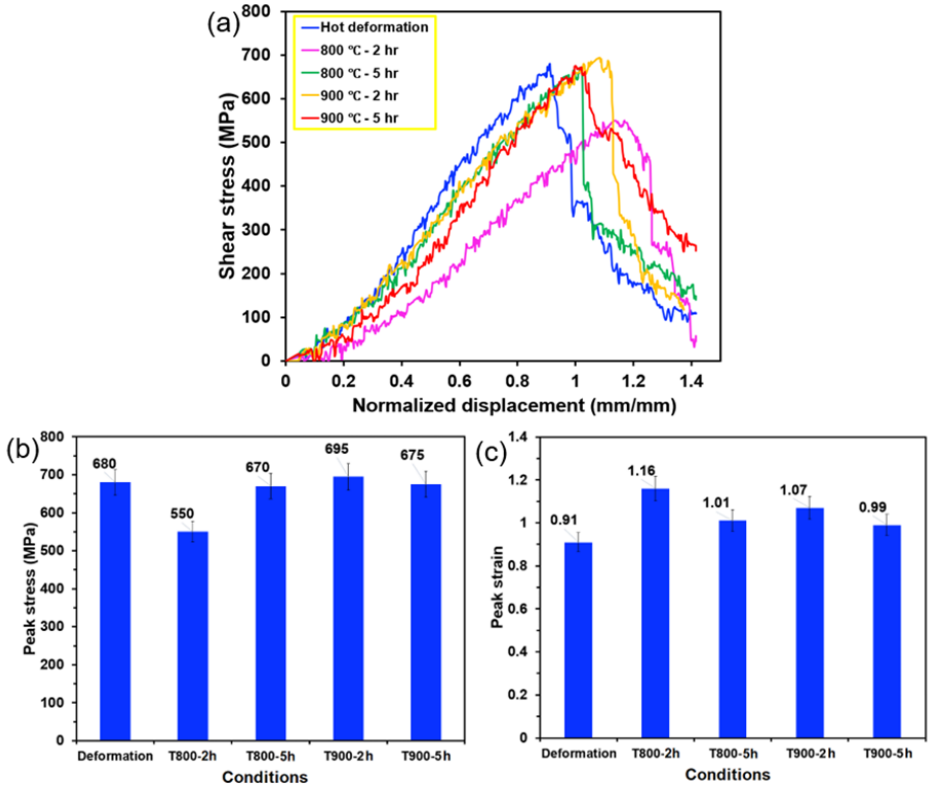

Fig. 15. (a) The engineering τ-δ curves of Ti-811 alloy during SPT and (b, c) the maximum values of stress and strain at different conditions, respectively.

cracking, due to reduced stress concentration at the α/β interface, and increased deformability of globular α particles [45-47].

It can be concluded that at this temperature and heat treatment time, the reduction in the size of the layers and the formation of globular α particles lead achieving the maximum strength and the highest elongation. With increasing heat treatment time at 900 °C, grain growth and a reduction in the density of grain boundaries and α/β interfaces reduce the barriers to crack propagation, resulting in decreased mechanical performance [48, 49].

4. Conclusions

In this study, the globularization behavior of the α phase and the mechanical properties of Ti-811 alloy with an initial lamellar structure were investigated after hot deformation (at 1000 °C and 0.001 s^{-1}) and heat treatment in the temperature range of 800-900 °C for different holding times ranging from 1 h to 5 h. The most important results of this study can be summarized as follows:

1) Hot deformation of the homogenized Ti-811 alloy in the α + β region resulted in an increase in the thickness of the α layers and the formation of a low fraction of globular α particles.
2) The microstructural results showed that the fraction of globular α particles increased with increasing heat treatment temperature and time. By increasing temperature from 800 °C to 900 °C for 5 h, the aspect ratio of α particles decreased from 7.2 to 6.2 and the fraction of globular α phase increased from 68% to 79%.
3) With increasing heat treatment temperature from 800 °C to 900 °C, the globularization mechanism changed from boundary splitting to Ostwald growth and interface migration. Static globularization kinetics of Ti-811 alloy was well modeled by the modified JMAK at 900 °C.
4) The maximum shear stress and elongation of heat-treated Ti-811 alloy were obtained at 900 °C for a holding time of 2 h, due to the presence of a suitable microstructure of the α phase.

Authors' contributions

G. Ebrahimi: Supervision, Writing - review & editing

Z. Mirzaie: Formal analysis, Investigation, Writing original draft

H. Ezatpour: Writing original draft - review & editing

Conflict of interest

The authors have no relevant financial or non-financial interests to disclose.

Funding

This research received no external funding.

Data availability

The data will be made available upon request.

5. References

[1] Shean Lee, R., & Chang Lin, H. (1998). Process design based on the deformation mechanism for the non-isothermal forging of Ti–6Al–4V alloy. *Journal of Materials Processing Technology*, *79*(1), 224-235. https://doi.org/10.1016/S0924-0136(98)00016-8

[2] Qi, Y., Wang, X., Tian, P., Zhuang, W., Li, Y., Chu, Z., Ding, X., & Sun, J. (2025). Explosive compression strengthened a near-α titanium alloy with high strength. *Journal of Alloys and Compounds*, *1030*, 180896. https://doi.org/10.1016/j.jallcom.2025.180896

[3] Jiang, X. J., Zhang, L. W., Sun, G. W., Yang, J. H., Ran, Q. X., & Wu, H. Y. (2023). Excellent mechanical properties of a Ti-based alloy via optimizing grain boundary α phase. *Materials Letters*, *333*, 133662. https://doi.org/10.1016/j.matlet.2022.133662

[4] Zarghani, F., Ebrahimi, G. R., Taheri, J., & Ezatpour, H. R. (2023). Hot compressive deformation behavior of Ti-8Al-1Mo-1V titanium alloy at elevated temperatures: Focus on flow behavior, constitutive modeling, and processing maps. *Materials Today Communications*, *37*, 107235. https://doi.org/10.1016/j.mtcomm.2023.107235

[5] Ding, Z., & Jiao, Z. B. (2021). Metallic materials for making multi-scaled metallic parts and structures. *Encyclopedia of Materials: Metals and Alloys*, *4*, 19-36. https://doi.org/10.1016/B978-0-12-819726-4.00007-7

[6] Shi, X., Zeng, W., Long, Y., & Zhu, Y. (2017). Microstructure evolution and mechanical properties of near-α Ti-8Al-1Mo-1V alloy at different solution

temperatures and cooling rates. *Journal of Alloys and Compounds*, *727*, 555-564. https://doi.org/10.1016/j.jallcom.2017.08.165

[7] Lin, X., Huang, H., Yuan, X., Wang, Y., Zheng, B., Zuo, X., & Zhou, G. (2022). Study on hot deformation behavior and processing map of a Ti-47.5Al-2.5V-1.0Cr-0.2Zr alloy with a fully lamellar microstructure. *Journal of Alloys and Compounds*, *901*, 163648. https://doi.org/10.1016/j.jallcom.2022.163648

[8] Seshacharyulu, T., Medeiros, S. C., Morgan, J. T., Malas, J. C., Frazier, W. G., & Prasad, Y. V. R. K. (2000). Hot deformation and microstructural damage mechanisms in extra-low interstitial (ELI) grade Ti–6Al–4V. *Materials Science and Engineering: A*, *279*(1), 289-299. https://doi.org/10.1016/S0921-5093(99)00173-2

[9] Yang-huan-zi, L., Ji, G., & Min, S. (2024). Phase transformation in titanium alloys: A review. *Transactions of Nonferrous Metals Society of China*, *34*(10), 3093-3117. https://doi.org/10.1016/S1003-6326(24)66597-0

[10] Xu, J., Zeng, W., Ma, H., & Zhou, D. (2018). Static globularization mechanism of Ti-17 alloy during heat treatment. *Journal of Alloys and Compounds*, *736*, 99-107. https://doi.org/10.1016/j.jallcom.2017.11.117

[11] Xu, J., Zeng, W., Jia, Z., Sun, X., & Zhou, J. (2014). Static globularization kinetics for Ti-17 alloy with initial lamellar microstructure. *Journal of Alloys and Compounds*, *603*, 239-247. https://doi.org/10.1016/j.jallcom.2014.03.082

[12] Abbasi, S. M., & Momeni, A. (2011). Effect of hot working and post-deformation heat treatment on microstructure and tensile properties of Ti-6Al-4V alloy *Transactions of Nonferrous Metals Society of China*, *21*(8), 1728-1734. https://doi.org/10.1016/S1003-6326(11)60922-9

[13] Rani, S. U., Kesavan, D., & Kamaraj, M. (2023). Possible globularization mechanism in LPBF additively manufactured Ti-6Al-4V alloys. *Materials Characterization*, *205*, 113303. https://doi.org/10.1016/j.matchar.2023.113303

[14] Wang, K., Zeng, W., Zhao, Y., Lai, Y., & Zhou, Y. (2010). Dynamic globularization kinetics during hot working of Ti-17 alloy with initial lamellar microstructure. *Materials Science and Engineering: A*, *527*(10), 2559-2566. https://doi.org/10.1016/j.msea.2010.01.034

[15] Stefansson, N., Semiatin, S. L., & Eylon, D. (2002). The kinetics of static globularization of Ti-6Al-4V. *Metallurgical and Materials Transactions A*, *33*(11), 3527-3534. https://doi.org/10.1007/s11661-002-0340-x

[16] Park, C. H., Won, J. W., Park, J. W., Semiatin, S. L., & Lee, C. S. (2012). Mechanisms and kinetics of static spheroidization of hot-worked Ti-6Al-2Sn-4Zr-2Mo-0.1Si with a lamellar microstructure. *Metallurgical and Materials Transactions A*, *43*(3), 977-985. https://doi.org/10.1007/s11661-011-1019-y

[17] Stefansson, N., & Semiatin, S. (2003). Mechanisms of globularization of Ti-6Al-4V during static heat treatment. *Metallurgical and Materials Transactions A*, *34*(3), 691-698. https://doi.org/10.1007/s11661-003-0103-3

[18] Chong, Y., Bhattacharjee, T., Gholizadeh, R., Yi, J., & Tsuji, N. (2019). Investigation on the hot deformation behaviors and globularization mechanisms of lamellar Ti–6Al–4V alloy within a wide range of deformation temperatures. *Materialia*, *8*, 100480. https://doi.org/10.2139/ssrn.3438562

[19] Zherebtsov, S., Murzinova, M., Salishchev, G., & Semiatin, S. (2011). Spheroidization of the lamellar microstructure in Ti–6Al–4V alloy during warm deformation and annealing. *Acta Materialia*, *59*(10), 4138-4150. https://doi.org/10.1016/j.actamat.2011.03.037

[20] Cakan, B. C., Soyarslan, C., Bargmann, S., & Hahner, P. (2017). Experimental and computational study of ductile fracture in small punch tests, *Metlas*, *10*(10), 1185. https://doi.org/10.3390/ma10101185

[21] Skripnyak, V. V., Iohim, K. V., & Skripnyak, V. A. (2023). Mechanical behavior of titanium alloys at moderate strain rates characterized by the punch test technique. *Materials*, *16*(1), 416. https://doi.org/10.3390/ma16010416

[22] Torres, J., & Gordon, A. P. (2021). Mechanics of the small punch test: a review and qualification of additive manufacturing materials. *Journal of Materials Science*, *56*(18), 10707-10744. https://doi.org/10.1007/s10853-021-05929-8

[23] Fu, Q., Yuan, W., & Xiang, W. (2021). Dynamic softening mechanisms and microstructure evolution of TB18 titanium alloy during uniaxial hot deformation. *Metals*, *11*, 789. https://doi.org/10.3390/met11050789

[24] Mutombo, K., Siyasiya, C., & Stumpf, W. E. (2014). Dynamic globularization of α-phase in Ti6Al4V alloy during hot compression. *Materials Science Forum*, *783-786*, 584-590. https://doi.org/10.4028/www.scientific.net/MSF.783-786.584

[25] Zhou, C., Cao, F., Yang, Z., & Rao, W. (2024). Dynamic recrystallization constitutive model and texture evolution of metastable β titanium alloy TB8 during thermal deformation. *Materials*, *17*(7), 1572. https://doi.org/10.3390/ma17071572

[26] Ezatpour, H. R., Torabi Parizi, M., Ebrahimi, G. R., & Huo, Y. (2023). Punching shear failure behavior of fine-grained ZK60 Mg alloy processed by a novel forward shear normal extrusion process at room and elevated temperatures. *Engineering Failure Analysis*, *153*, 107568. https://doi.org/10.1016/j.engfailanal.2023.107568

[27] Alizadeh, R., & Mahmudi, R. (2010). Evaluating high-temperature mechanical behavior of cast Mg-4Zn-xSb magnesium alloys by shear punch testing. *Materials Science and Engineering: A*, *527*(16), 3975-3983. https://doi.org/10.1016/j.msea.2010.03.007

[28] Yu, Y., Qiang, F., Cai, J., Li, C., Wang, W., & Wang, K. (2025). Hot deformation behavior and microstructural evolution of as-cast TC4 titanium alloy. *Journal of Materials Science*, *60*(21), 8870-8889. https://doi.org/10.1007/s10853-025-10938-y

[29] Wang, X., Liu, P., Liang, C., Lu, T., Feng, T., Niu, H., Dong, Y., & Liu, X. (2024). Investigation on the thermal deformation mechanisms and constitutive model of Ti-55511 titanium alloy. *Journal of Materials Research and Technology*, *33*, 6780-6797. https://doi.org/10.1016/j.jmrt.2024.11.057

[30] Jonas, J. J., Aranas, C., Fall, A., & Jahazi, M. (2017). Transformation softening in three titanium alloys. *Materials & Design*, *113*, 305-310. https://doi.org/10.1016/j.matdes.2016.10.039

[31] Yu, J., Li, Z., Qian, C., Huang, S., & Xiao, H. (2023). Investigation of deformation behavior, microstructure evolution, and hot processing map of a new near-α Ti alloy. *Journal of Materials Research and Technology*, *23*, 2275-2287. https://doi.org/10.1016/j.jmrt.2023.01.177

[32] Wanjara, P., Jahazi, M., Monajati, H., Yue, S., & Immarigeon, J. P. (2005). Hot working behavior of near-α alloy IMI834. *Materials Science and Engineering: A*, *396*(1-2), 50-60. https://doi.org/10.1016/j.msea.2004.12.005

[33] Zhang, Z. X., Qu, S. J., Feng, A. H., Shen, J., & Chen, D. L. (2017). Hot deformation behavior of Ti-6Al-4V alloy: effect of initial microstructure. *Journal of Alloys and Compounds*, *718*, 170-181. https://doi.org/10.1016/j.jallcom.2017.05.097

[34] Ezatpour, H. R., Ebrahimi, G. R., & Zarghani, F. (2024). Effect of processing parameters on the morphology of α-phase in Ti-6Al-4V alloy during the two-step hot deformation. *Iranian Journal of Materials Forming*, *10*(3), 54-62. https://doi.org/10.22099/ijmf.2024.49049.1277

[35] Ebrahimi, G. R., Zarghani, F., Ezatpour, H. R., & Taheri, J. (2024). Hot working behaviour of Ti–8Al–1Mo–1V alloy through the hot compression test. *Materials Science and Technology*, *40*(10), 755-765. https://doi.org/10.1177/02670836231223807

[36] Gao, P., Fu, M., Zhan, M., Lei, Z., & Li, Y. (2020). Deformation behavior and microstructure evolution of titanium alloys with lamellar microstructure in hot working process: a review. *Journal of Materials Science & Technology*, *39*, 56-73. https://doi.org/10.1016/j.jmst.2019.07.052

[37] Li, H., Zhao, Z., Guo, H., Yao, Z., Ning, Y., Miao, X., & Ge, M. (2017). Effect of initial alpha lamellar thickness on deformation behavior of a near-α high-temperature alloy during thermomechanical processing. *Materials Science and Engineering: A*, *682*, 345-353. https://doi.org/10.1016/j.msea.2016.11.063

[38] Li, H., Zhao, Z., Ning, Y., Guo, H., & Yao, Z. (2018). Characterization of microstructural evolution for a near-α titanium alloy with different initial lamellar microstructures. *Metals*, *8*(12), 1045. https://doi.org/10.3390/met8121045

[39] Wu, C. b., Yang, H., Fan, X. g., & Sun, Z. c. (2011). Dynamic globularization kinetics during hot working of TA15 titanium alloy with colony microstructure. *Transactions of Nonferrous Metals Society of China*, *21*(9), 1963-1969. https://doi.org/10.1016/S1003-6326(11)60957-6

[40] Song, H. W., Zhang, S. H., & Cheng, M. (2009). Dynamic globularization kinetics during hot working of a two phase titanium alloy with a colony alpha microstructure. *Journal of Alloys and Compounds*, *480*(2), 922-927. https://doi.org/10.1016/j.jallcom.2009.02.059

[41] Ma, X., Zeng, W., Tian, F., & Zhou, Y. (2012). The kinetics of dynamic globularization during hot working of a two phase titanium alloy with starting lamellar microstructure. *Materials Science and Engineering: A*, *548*, 6-11. https://doi.org/10.1016/j.msea.2012.03.022

[42] Chen, H., & Cao, C. (2011). Static globularization of TC11 alloy during hot working process. *Rare Metal Materials and Engineering*, *40*(6), 946-950. https://doi.org/10.1016/S1875-5372(11)60038-6

[43] Fan, X. G., Yang, H., Yan, S. L., Gao, P. F., & Zhou, J. H. (2012). Mechanism and kinetics of static globularization in TA15 titanium alloy with transformed structure. *Journal of Alloys and Compounds*, *533*, 1-8. https://doi.org/10.1016/j.jallcom.2012.03.113

[44] Pang, H. y., Luo, J., Zhang, Z. g., Han, W. c., Xu, K. f., & Li, M. q. (2022). Quantitative analysis of globularization and modeling of TC17 alloy with basketweave microstructure. *Transactions of Nonferrous Metals Society of China*, *32*(3), 850-867. https://doi.org/10.1016/S1003-6326(22)65838-2

[45] Zhang, J., Li, H., & Zhan, M. (2020). Review on globularization of titanium alloy with lamellar colony. *Manufacturing Review*, *7*, 18. https://doi.org/10.1051/mfreview/2020015

[46] Zhang, J., Li, H., Sun, X., & Zhan, M. (2020). A multi-scale MCCPFEM framework: Modeling of thermal interface grooving and deformation anisotropy of titanium alloy with lamellar colony. *International Journal of Plasticity*, *135*, 102804. https://doi.org/10.1016/j.ijplas.2020.102804

[47] Shugurov, A. (2021). Microstructure and mechanical properties of titanium alloys. *Metals*, *11*(10), 1617. https://doi.org/10.3390/met11101617

[48] Liu, K., Zhang, H., Xiu, M., Huang, Z., Huang, H., Xu, Y., Zhou, R., & Xiao, H. (2023). Microstructure evolution, mechanical properties, and corrosion resistance of hot rolled and annealed Ti-Mo-Ni alloy. *Metals*, *13*(3), 566. https://doi.org/10.3390/met13030566

[49] Majchrowicz, K., Sotniczuk, A., Malicka, J., Choińska, E., & Garbacz, H. (2023). Thermal stability and mechanical behavior of ultrafine-grained titanium with different impurity content. *Materials (Basel)*, *16*(4). https://doi.org/10.3390/ma16041339